

1 Generic Behavior of Ultrastability and Anisotropic Molecular 2 Packing in Codeposited Organic Semiconductor Glass Mixtures

3 Shinian Cheng, Yejung Lee, Junguang Yu, Lian Yu, and Mark D. Ediger*



Cite This: <https://doi.org/10.1021/acs.chemmater.3c02935>



Read Online

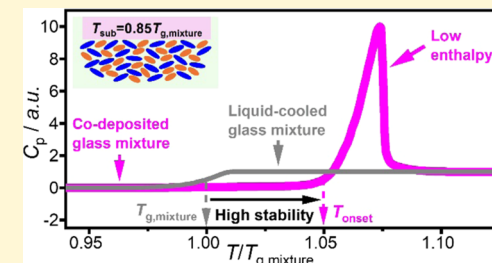
ACCESS |

Metrics & More

Article Recommendations

Supporting Information

4 **ABSTRACT:** Vapor-deposited glass mixtures of organic semiconductors
5 commonly serve as active layers in organic electronic devices, whose lifetime
6 and performance are strongly influenced by the stability and structure of these
7 mixed glasses. Here, we study the stability and anisotropic molecular packing of six
8 codeposited organic semiconductor glass mixtures with a 50:50 weight ratio by
9 differential scanning calorimetry and spectroscopic ellipsometry. We find that all
10 six binary systems exhibit high kinetic stability and significantly reduced enthalpy
11 relative to the corresponding liquid-cooled glassy mixtures (ultrastable behavior),
12 even for systems where the glass-transition temperatures of the components differ
13 by more than 90 K. Furthermore, we demonstrate that the birefringence of a
14 codeposited glass mixture, a measure of its anisotropic packing, can be predicted from the birefringence of glasses of the two pure
15 components. These results for stability and structure are expected to be applicable to other codeposited organic semiconductor glass
16 mixtures, so long as the two components mix well in the glass and individually can form ultrastable glasses. Therefore, our findings
17 are significant for the design of novel electronic devices with enhanced device lifetime and increased operational efficiency.



18 ■ INTRODUCTION

19 Glasses are noncrystalline materials that are widely used in
20 applications where macroscopic homogeneity and smooth
21 surfaces are required. For example, organic semiconductor
22 glasses are utilized as active layers to ensure uniform
23 performance in organic light-emitting diode (OLED) displays
24 that are being used in cellphones and televisions.¹ However, as
25 nonequilibrium materials, glasses can evolve with time through
26 physical aging,² crystallization,³ and degradation,⁴ which can
27 lead to a loss of device performance.⁴ Recent studies have
28 shown that glasses prepared by physical vapor deposition
29 (PVD) can exhibit exceptional kinetic and thermodynamic
30 stability (ultrastable behavior)^{5,6} that can overcome many of
31 these challenges,^{7–9} broadening their potential use in
32 applications. In addition, PVD glasses can exhibit anisotropic
33 packing,^{10–12} and the molecular orientation can be continu-
34 ously tuned from “standing up” to “lying down” relative to the
35 substrate through varying deposition conditions.¹³ While most
36 past work has focused on single-component PVD organic
37 glasses,^{8,14} devices typically utilize multicomponent PVD
38 glasses, and our understanding of multicomponent systems is
39 much more limited.

40 One major challenge is to understand the conditions under
41 which codeposited glasses can exhibit the very high kinetic
42 stability of single-component PVD glasses.⁵ Previous studies
43 on single-component PVD glasses have demonstrated that high
44 surface mobility below the glass-transition temperature (T_g) is
45 the key to forming ultrastable glasses.⁵ The surface
46 equilibration mechanism explains that mobility near the
47 surface allows newly deposited molecules to find low energy

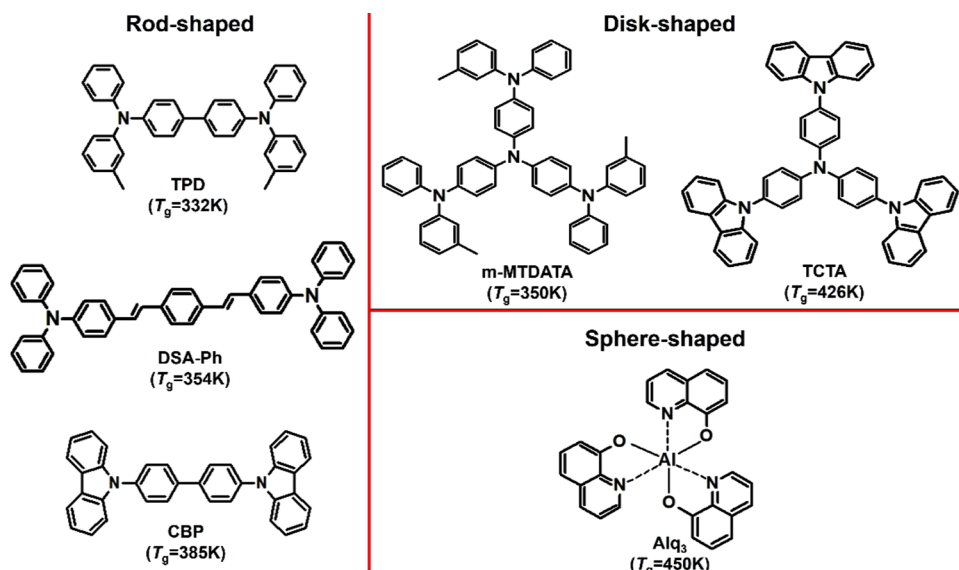
48 and highly stable packing arrangements that are then locked
49 into place by subsequent deposition. From this perspective,
50 highly stable codeposited glass mixtures might be expected at
51 deposition conditions, where both components can individu-
52 ally form ultrastable single-component PVD glasses. Recent
53 reports on PVD glass mixtures of isomers¹⁵ and a pair of
54 organic semiconductors with similar T_g values¹⁶ support this
55 viewpoint. However, it is unclear whether this result holds
56 generically for organic semiconductors. For example, would
57 codeposition of molecules with a large difference in T_g values
58 form ultrastable PVD glass mixtures, since it may be impossible
59 to find a deposition temperature, where both components have
60 high surface mobility?

61 A second important challenge is to understand and control
62 the molecular orientation in multicomponent PVD organic
63 glasses. As one example where this is important, the light-
64 emitting layers in OLEDs are PVD glass mixtures, in which an
65 emitter is dispersed in a host.¹⁷ The molecular orientation of
66 emitter molecules affects the emission of light from thin films
67 and, thereby, the device efficiency. Recent work has
68 demonstrated that a horizontal molecular orientation of the
69 transition dipole of light emitters can increase device efficiency

Received: November 17, 2023

Revised: March 13, 2024

Accepted: March 15, 2024

Scheme 1. Chemical Structures and Glass-Transition Temperatures (T_g) of the Organic Semiconductors Studied Here^a

^aThe T_g is determined from DSC measurements in a heating process with 10 K/min (except for CBP, where 50 K/min was utilized³²). T_g values for TPD and m-MTDATA are taken from ref 16 DSC results for DSA-Ph, TCTA, and Alq₃ are given in the Supporting Information (SI).

70 by at least a factor of 1.3, relative to random emitter
 71 orientations.^{18–20} Previous work on emitter orientation has
 72 identified the shape of the emitter molecule^{21,22} and the glass-
 73 transition temperature of the host^{22–24} as key variables, and
 74 much of this work^{23,25,26} is consistent with the surface
 75 equilibration mechanism. Another example of the importance
 76 of molecular orientation in multicomponent PVD glasses is the
 77 orientation of polar molecules, which determines the surface
 78 charge (or giant surface potential, GSP²⁷), and this can have a
 79 major influence on charge injection in devices.^{28,29} Recent
 80 work maximized the surface charge by adjusting the substrate
 81 temperature and deposition rate, in qualitative accord with the
 82 surface equilibration mechanism.^{30,31} These examples illustrate
 83 that it is practically important to understand and control the
 84 molecular orientation in two-component PVD glasses of
 85 organic semiconductors.

86 Here, we perform a thorough survey of the stability and
 87 molecular orientation of six binary vapor-deposited organic
 88 semiconductor glass mixtures with a 50:50 mass concentration.
 89 This regime in the middle of the composition space is
 90 anticipated to be the most challenging to understand. Scheme
 91 shows the chemical structures and calorimetric glass-
 92 transition temperatures (T_g) of the studied organic semi-
 93 conductors. To ensure the diversity of studied mixtures, the
 94 selected compounds cover a broad range of T_g values (from
 95 332 to 450 K) and different molecular shapes, including rod-,
 96 disk-, and sphere-shaped molecules. By using differential
 97 scanning calorimetry (DSC), we evaluate the enthalpy and
 98 kinetic stability of these codeposited glass mixtures of organic
 99 semiconductors at substrate temperatures, $T_{\text{sub}} = 0.78–$
 100 $0.88T_{g,\text{mixture}}$; this is the temperature window, where the most
 101 stable single-component PVD organic semiconductor glasses
 102 are obtained. The results show that all six codeposited glass
 103 mixtures exhibit high kinetic stability and low enthalpy,
 104 comparable to the most stable single-component PVD organic
 105 glasses. This high stability and low enthalpy are observed even
 106 when the difference in pure component T_g values exceeds 90
 107 K. In addition, the molecular orientation of the binary glasses

108 deposited across a wide range of T_{sub} is investigated using
 109 variable angle spectroscopic ellipsometry (VASE) to obtain the
 110 birefringence; in mixed glasses, the birefringence contains
 111 information about the orientation of both components. We
 112 find that for all six binary mixtures, the birefringence is
 113 controlled by $T_{\text{sub}}/T_{g,\text{mixture}}$, akin to that in single-component
 114 PVD organic glasses. Furthermore, we show that the
 115 birefringence of a binary PVD glass mixture can be predicted
 116 from the birefringence of the neat PVD glasses of the two
 117 components through a model derived from the surface
 118 equilibration mechanism.

■ EXPERIMENTAL METHODS

Materials. TPD (*N,N'*-Bis(3-methylphenyl)-*N,N'*-diphenylbenzidine, 99%), CBP (4,4'-Bis(*N*-carbazolyl)-1,1'-biphenyl, 99.9%), *m*-MTDATA (4,4',4''-Tris[phenyl(*m*-tolyl)amino]triphenylamine, 98.7%), TCTA (Tris(4-carbazoyl-9-ylphenyl)amine, >97%), and Alq₃ (Tris(8-hydroxyquinoline) aluminum, 99.9%) were purchased from Sigma-Aldrich. DSA-Ph (1-(4-Di-[4-(*N,N*-diphenyl)amino]-styryl-benzene, 99%) was purchased from Luminescence Technology Corporation. All compounds were used without further purification.

PVD Glass Mixture Preparation. Codeposited glass mixtures were prepared in a vacuum chamber with a base pressure of $\sim 10^{-6}$ Torr. The deposition rate for each component was controlled individually by heating two independent crucibles using resistive wire heaters. By setting the same deposition rate for the two components, we prepared PVD glass mixtures with a 50:50 mass ratio of components. The total deposition rate was 0.42 ± 0.02 nm/s and monitored using a quartz crystal microbalance (QCM). The thickness of the deposited films was measured by the QCM. The substrate temperature was held constant during deposition using a Lakeshore controller with platinum RTD sensors. Codeposited glassy films with a thickness of 1400 nm were deposited onto 120 nm thick gold foil (purchased from Barnabas Gold) for differential scanning calorimetry measurements, while films with a thickness of 380–400 nm for spectroscopic ellipsometry measurements were deposited onto one-side polished silicon wafers (purchased from Virginia Semiconductor).

Differential Scanning Calorimetry (DSC) Measurements. Thermal analysis of bulk and codeposited samples was performed using a TA Q2000 differential scanning calorimeter (New Castle,

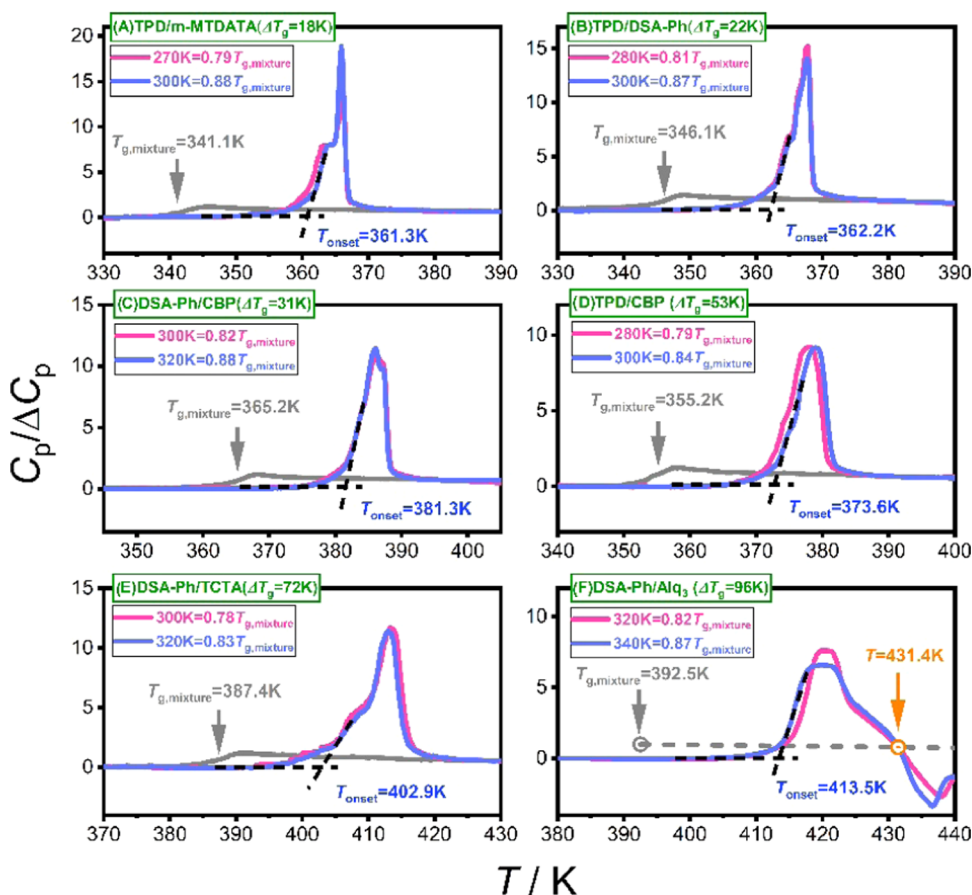


Figure 1. DSC results for six 50:50 binary mixtures of organic semiconductors. The pink and blue curves present the results of codeposited glass mixtures with the substrate temperatures given in the legend, and gray curves denote results for the corresponding liquid-cooled glass mixtures. For panel (F), the heat capacity of the supercooled liquid of DSA-Ph/Alq₃ is predicted according to the procedure given in the SI.

148 DE). To determine the kinetic stability and enthalpy of codeposited
 149 glass mixtures, the as-deposited films with the attached gold foil (120
 150 nm thickness) were folded and loaded into a Tzero pan; the pan was
 151 sealed by a Tzero lid using a crimper press to achieve good contact
 152 between the tested sample and the pan. The scanning rate was 10 K/
 153 min for both heating and cooling processes under 50 mL/min N₂
 154 purge.

155 **Spectroscopic Ellipsometry Measurements.** The optical
 156 properties of codeposited glass mixtures were probed using
 157 spectroscopic ellipsometry (J.A. Woollam M-2000U). The optical
 158 parameters Ψ and Δ were determined in the wavelength range 600–
 159 1000 nm at room temperature through variable angle measurements
 160 at three incidence angles of 50, 60, and 70°. The anisotropic Cauchy
 161 model was applied to model the experimental data, determining the
 162 thickness and ordinary (n_0) and extraordinary (n_e) refractive indices.
 163 The birefringence ($\Delta n = n_e - n_0$) of codeposited glass mixtures was
 164 reported at a wavelength of 632.8 nm.

165 ■ RESULTS

166 **Kinetic Stability.** We employ differential scanning
 167 calorimetry (DSC) to evaluate the kinetic stability of
 168 codeposited glass mixtures of organic semiconductors. The
 169 obtained DSC results for six 50:50 binary systems are listed in
 170 Figure 1. The data are obtained during heating with a rate of
 171 10 K/min. The pink and blue curves present the calorimetric
 172 data for the as-deposited glass mixtures. After the as-deposited
 173 glasses were entirely transformed into the supercooled liquid
 174 state, the samples were cooled at 10 K/min to form liquid-
 175 cooled (LC) glasses. The gray curves denote the reheating

176 DSC results of the corresponding LC glass mixtures, from
 177 which the glass-transition temperature of the mixtures,
 178 $T_{g,mixture}$, was determined and is displayed in Figure 1. Notably,
 179 those of their corresponding bulk mixtures with a 50:50 mass
 180 ratio, as shown in Figure S2. The DSC result of the bulk TPD/
 181 m-MTADATA mixture can be found in ref 16. For each panel in
 182 Figure 1, the heat capacity is normalized to the heat capacity
 183 change, ΔC_p , of the liquid-cooled glass mixtures during the
 184 glass-to-liquid transition.

185 For every binary system of organic semiconductors
 186 considered, the kinetic stability of the codeposited glasses
 187 prepared at $T_{sub} = 0.78–0.88T_{g,mixture}$ is significantly enhanced,
 188 in comparison to the corresponding liquid-cooled glass. As
 189 shown in Figure 1, for each system, the onset temperature
 190 T_{onset} , where the PVD glass mixture starts to transform, is 15–
 191 21 K higher than the $T_{g,mixture}$ of the liquid-cooled glass. This is
 192 a straightforward indication that the codeposited glass mixtures
 193 prepared at these substrate temperatures are kinetically more
 194 stable since more thermal energy is required to dislodge the
 195 molecules from the solid-state packing formed by vapor
 196 deposition. For one of the six mixtures, a slightly different
 197 procedure was used; since the as-deposited DSA-Ph/Alq₃
 198 mixture crystallized during the glass-to-liquid transformation
 199 process, the $T_{g,mixture}$ and ΔC_p values of the DSA-Ph/Alq₃
 200 mixture could not be obtained directly. We estimate $T_{g,mixture} =$
 201 392.5 K for DSA-Ph/Alq₃ at a 10 K/min heating rate (4 K
 202 higher than the previously reported value obtained at 1 K/
 203

204 min³³) and $\Delta C_p = 0.369 \text{ K J}^{-1} \text{ g}^{-1}$ (the weighted average of 205 ΔC_p for pure DSA-Ph and pure Alq3). The detailed procedure 206 for estimating the heat capacity for the DSA-Ph/Alq3 liquid is 207 given in the *Supporting Information (SI)*. We infer that all as- 208 deposited mixtures studied here form a single homogeneous 209 glassy phase and the presence of a shoulder (or occasionally a 210 second peak) in the DSC response is not due to component 211 segregation, based upon two observations: (1) the shoulders/ 212 peaks are not completely reproducible. One example has been 213 presented in *Figure S4*; (2) for all mixtures, the DSC response 214 spans a narrow temperature interval around 8–15 K, which is 215 comparable to (but slightly larger than) the glass-transition 216 width for single-component PVD glasses (*Figure 2*). The

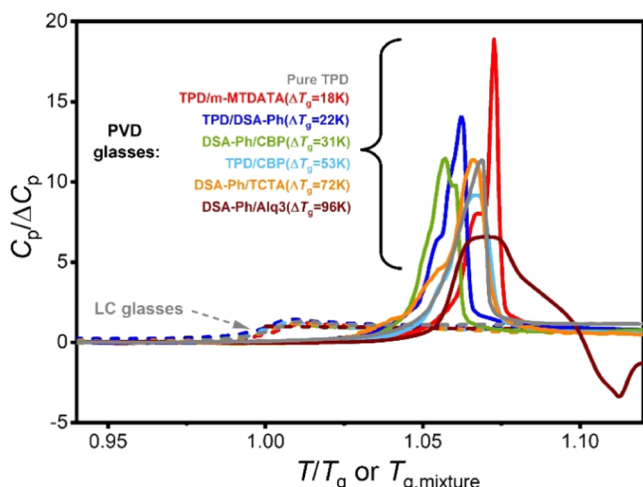


Figure 2. DSC heating results for a vapor-deposited (solid lines) and liquid-cooled (dashed lines) organic semiconductor glass mixture. The scanning temperature is normalized to the glass-transition temperature of the samples. Note, for each mixture, the DSC data of the sample deposited at the higher T_{sub} is displayed.

217 slightly wider transition width for the mixed glasses and the 218 presence of shoulder/peaks may arise from variations in 219 composition within the sample due to the fluctuations in 220 individual deposition rates and composition changes across 221 films due to the deposition chamber geometry.

222 In *Figure 2*, we compare the kinetic stability of these 223 codeposited glass mixtures with the most stable glass of pure 224 TPD¹⁶ (deposited at $T_{\text{sub}} = 0.86T_g$ and shown in gray); this 225 TPD data is representative of that obtained for single- 226 component PVD glasses of organic semiconductors.¹⁶ For 227 this purpose, we normalized the scanning temperature to the 228 glass-transition temperature of the liquid-cooled glasses. 229 Remarkably, for all six binary systems investigated, the 230 temperature where the vapor-deposited glass mixtures start 231 to transform is around 1.05 times higher than the 232 corresponding T_g value. As shown, this kinetic stability is 233 comparable to that of the most stable vapor-deposited TPD 234 glass. It is worth noting that the difference in glass-transition 235 temperatures of the two components, ΔT_g , is as large as 96 K, 236 which is five times larger than a recent work.¹⁶

237 **Enthalpy.** As shown in *Figure 2*, the codeposited glasses 238 show a pronounced endothermic peak during the glass-to- 239 liquid transition, while their corresponding liquid-cooled 240 glasses exhibit a step-like change in heat capacity with a 241 negligible endothermic peak. Similar to single-component 242 systems, this is an indication that the codeposited PVD glass

mixtures are low in energy landscape, akin to highly aged 243 glasses.⁵ The enthalpy of each PVD glass is obtained by 244 integrating the heat capacity curves in *Figure 1*, and these 245 results are shown in *Figure 3*. For all of the studied systems, 246 the enthalpy of codeposited glass mixtures is significantly lower 247 than that of the corresponding liquid-cooled glass mixtures. 248

We compare the enthalpies of different PVD glasses through 249 the use of fictive temperature T_f and we find that T_f for each of 250 the binary PVD glasses is much lower than $T_{g,\text{mixture}}$. The fictive 251 temperature T_f is frequently used to determine the extent to 252 which a glass is equilibrated. We determine T_f as the 253 temperature, where the enthalpy of the PVD glass meets the 254 extrapolation of the supercooled liquid enthalpy (dashed lines 255 in *Figure 3*). The T_f values for the PVD glasses are around 22– 256 40 K lower than $T_{g,\text{mixture}}$, indicating extraordinary thermody- 257 namic stability in codeposited mixtures. The uncertainty in the 258 determined T_f values is $\pm 3\text{ K}$, resulting from uncertainty in 259 extrapolating the supercooled liquid enthalpy to low temper- 260 atures. For context, we note that T_f for the most stable single- 261 component PVD glasses (i.e., TPD,^{16,34} TNB,⁵ and IMC³⁵) is 262 about 30 K lower than their T_g and similar results have been 263 reported for amber glasses aged for tens of millions of 264 years.^{36,37}

Comparison with Single-Component PVD Organic Glasses. The enhanced kinetic stability and reduced enthalpy 266 of these codeposited glass mixtures of organic semiconductors 267 are comparable to the most stable single-component organic 268 glasses. As shown in *Figures 4A,B*, for all codeposited glass 269 mixtures, the determined $T_{\text{onset}}/T_{g,\text{mixture}}$ values are between 270 1.04 and 1.06 (the gray shaded region in *Figure 4A*), and 272 simultaneously, the $T_f/T_{g,\text{mixture}}$ values are in the range of 0.90– 273 0.94 (the gray shaded region in *Figure 4B*). These values are 274 very similar to those for vapor-deposited single-component 275 systems (e.g., TPD shown here) prepared in the same T_{sub}/T_g 276 regime.^{13,38} This strongly supports the view that the kinetic 277 stability and enthalpy of PVD glass mixtures and neat glasses 278 are both controlled by the surface equilibration mechanism. 279 Furthermore, our results show that ultrastable glass mixtures 280 are generally obtained when deposited around $0.85T_{g,\text{mix}}$ 281 regardless of the molecular shape and T_g difference between 282 the two components.

Molecular Orientation. We employed spectroscopic 284 ellipsometry to study the average molecular orientation in 285 the six codeposited glass mixtures. The birefringence provides 286 an effective way to evaluate the average molecular orientation 287 and is defined as $\Delta n = n_e - n_0$ (where n_e and n_0 are the 288 extraordinary and ordinary indices of refraction, respectively).²⁸⁹ *Figure 5* shows the birefringence (red spherical points) 290 determined from spectroscopic ellipsometry for these binary 291 organic semiconductor glasses codeposited at $T_{\text{sub}}/T_{g,\text{mixture}} =$ 292 0.75–1.02.

All of the binary mixtures show similar trends in 294 birefringence when plotted as a function of $T_{\text{sub}}/T_{g,\text{mixture}}$. At 295 lower values of $T_{\text{sub}}/T_{g,\text{mixture}}$, all codeposited mixtures exhibit 296 significant negative birefringence, indicating a tendency toward 297 “face-on” packing. In contrast, isotropic PVD glass mixtures 298 with $\Delta n \approx 0$ are obtained when $T_{\text{sub}}/T_{g,\text{mixture}}$ is very near 299 unity. This indicates that $T_{\text{sub}}/T_{g,\text{mixture}}$ is a key factor in 300 controlling the molecular orientation of codeposited binary 301 organic semiconductor glasses. All binary mixtures studied here 302 have a 50:50 mass ratio of the two components, except for the 303 DSA-Ph/Alq3 mixtures with 58% DSA-Ph and 42% Alq3, as 304 reported in ref 33.³³

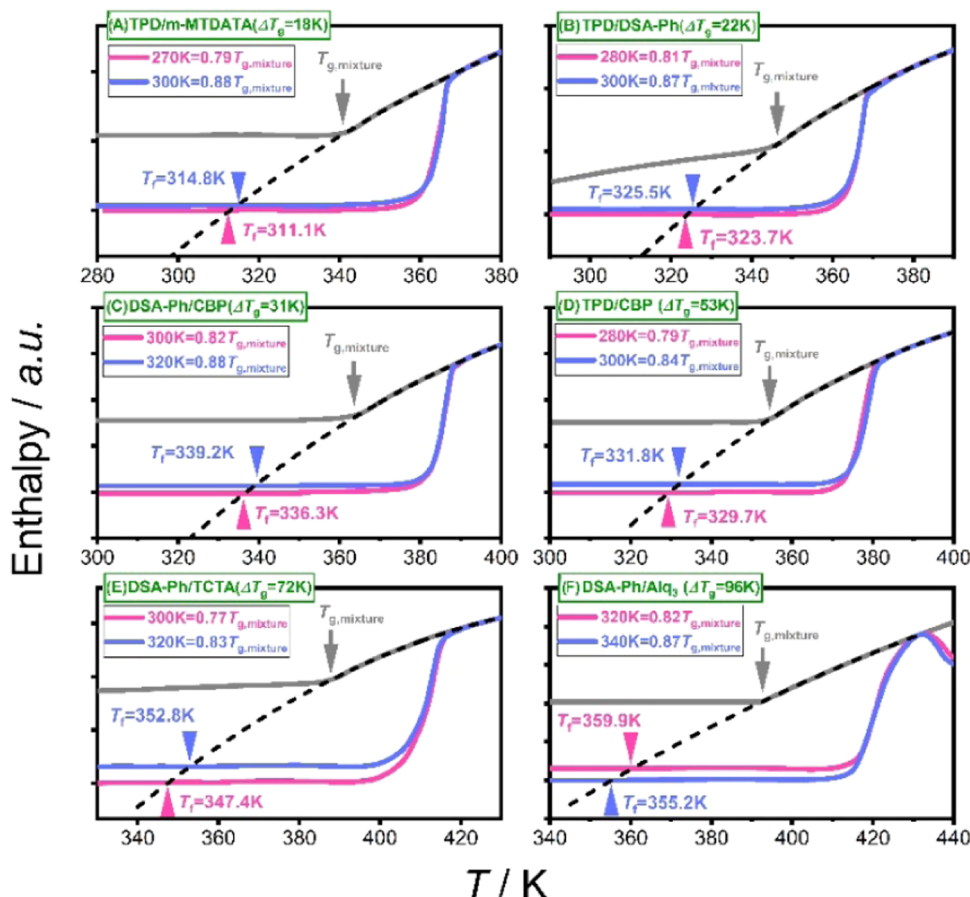


Figure 3. Enthalpy is plotted as a function of temperature for six codeposited glass mixtures (pink and blue) and corresponding liquid-cooled glass mixtures (gray). Dashed lines represent quadratic fits to the enthalpy data in the equilibrium liquid and extrapolation to lower temperature. Fictive temperatures (T_f) are determined by the intersection of the PVD glass enthalpy with the extrapolated supercooled liquid enthalpy.

306 We find that the birefringence of the codeposited glass
 307 mixtures can be quantitatively predicted. Specifically, for a
 308 given glass mixture AB, the observed birefringence is the
 309 weighted average of the pure glasses' birefringence obtained
 310 under the "iso-mobility" deposition condition

$$311 \frac{T_{\text{sub},AB}}{T_{g,AB}} = \frac{T_{\text{sub},A}}{T_{g,A}} = \frac{T_{\text{sub},B}}{T_{g,B}}$$

$$312 \Delta n_{AB} \left(\frac{T_{\text{sub},AB}}{T_{g,AB}} \right) = \varphi_A \times \Delta n_A \left(\frac{T_{\text{sub},A}}{T_{g,A}} \right) + \varphi_B \times \Delta n_B \left(\frac{T_{\text{sub},B}}{T_{g,B}} \right) \quad (1)$$

313 where Δn_{AB} , Δn_A , and Δn_B denote the birefringence of PVD
 314 glass mixture AB, pure glass A, and pure glass B; and φ_A and φ_B
 315 are the volume fractions of component A and component B in the
 316 mixture. **Equation 1** does not simply compute the average
 317 birefringence for a given substrate temperature (see **Discussion**
 318 section below). Rather, as an example, the birefringence of a
 319 mixture deposited at $0.8T_{g,\text{mixture}}$ is computed from the
 320 birefringence of component A deposited at $0.8T_{g,A}$ and the
 321 birefringence of component B deposited at $0.8T_{g,B}$. In our
 322 analysis, we assume that the volume fraction is equal to the
 323 weight fraction for PVD organic glasses.

324 Remarkably, the calculated birefringence (black solid lines in
 325 **Figure 5**) matches quite well with the experimental
 326 determinations (red spheres) for all six codeposited organic
 327 semiconductor glass mixtures. This result again emphasizes
 328 that the $T_{\text{sub}}/T_{g,\text{mixture}}$ is a key factor controlling the molecular

329 orientation of codeposited organic semiconductor glass
 330 mixtures, in analogy to single-component PVD organic glasses. 330

■ DISCUSSION

332 **Stability of Codeposited Semiconductor Glasses.** 332
 333 Here, we studied codeposited organic semiconductor mixtures 333
 334 with various molecular shape combinations and with ΔT_g for 334
 335 the two components up to 96 K. We found that all six glass 335
 336 mixtures exhibit highly enhanced kinetic stability and 336
 337 significantly reduced enthalpy when codeposited at $T_{\text{sub}} = 337$
 338 $0.78-0.88T_{g,\text{mixture}}$, comparable to the most stable single- 338
 339 component organic glasses. This is the first experimental 339
 340 evidence that stable glass formation is general for organic 340
 341 semiconductor mixtures even when ΔT_g is nearly 100 K. 341

342 These new results can be successfully interpreted by 342
 343 extending the surface equilibration mechanism⁵ to account 343
 344 for surface mobility in mixed systems. The surface equilibration 344
 345 mechanism emphasizes that high molecular mobility within 1– 345
 346 2 nm of the surface is the key for forming ultrastable PVD 346
 347 glasses since this allows molecules to reach (or nearly reach) 347
 348 equilibrium states at temperatures lower than the glass- 348
 349 transition temperature before they are buried by further 349
 350 deposition. For a codeposited mixture, we expect that both 350
 351 components must have high surface mobility in order to form 351
 352 an ultrastable glass. In a previous publication,¹⁶ we assumed 352
 353 that the surface mobility of a component is only determined by 353
 354 temperature (and not influenced by composition). We showed 354
 355 that this scenario could (just barely) explain ultrastable glass 355

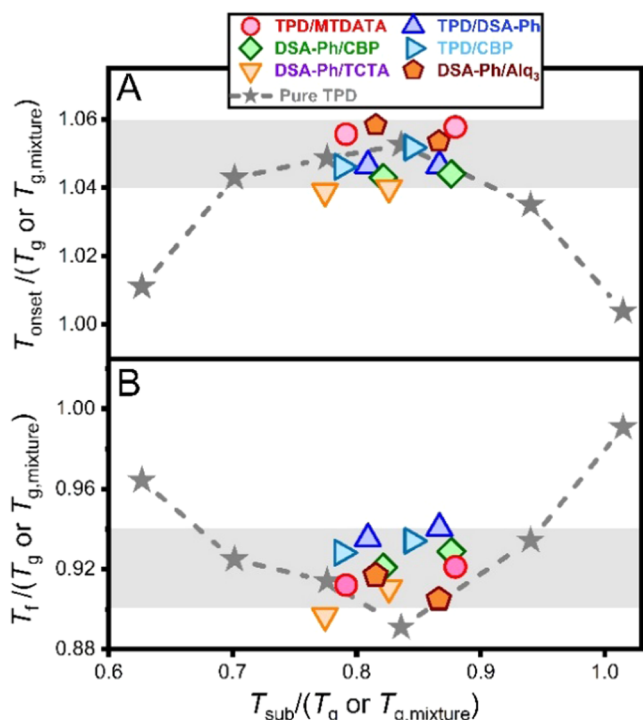


Figure 4. Kinetic stability (A) and enthalpy (B) of codeposited glass mixtures of organic semiconductors in comparison to a single-component system. Results are presented as a function of the substrate temperature during deposition. The dashed lines connect data for single-component PVD glasses of the TPD.

formation for $\Delta T_g = 18$ K. However, this scenario cannot explain ultrastable glass formation when ΔT_g is large since the high- T_g component would have very little mobility at $0.85T_{g,mixture}$. To explain our results, we infer that the surface mobility of each component is strongly influenced by composition, in addition to temperature, so that the two components have similar surface relaxation times (i.e., similar mobility) on top of the codeposited glass. By analogy, we note that the bulk glass transition has this character. If two molecules with different T_g values form a single liquid phase, a single, intermediate T_g value is usually observed,³⁹ indicating that the two molecules have similar mobilities in the mixture. With this inference that the surface mobility of each component is similar on top of the codeposited glass, the kinetic and thermodynamic stabilities of well-mixed codeposited glasses are naturally very similar to the behavior of ultrastable, single-component PVD glasses, as shown in Figure 4. The surface mobility of mixed glasses has rarely been studied,⁴⁰ and an experimental test of our inference is an important goal for future work.

The results of this study complement and extend the five previous literature reports of the kinetic and thermodynamic stability of multicomponent organic glasses. Two of these studies showed that mixtures of isomers (*cis*-/trans-decahydronaphthalene⁴¹ and *cis*-/trans-decahydroisoquinoline¹⁵) with identical glass-transition temperatures can form highly stable glasses. Qiu et al.⁴² showed that vapor-deposited dilute glass mixtures of 5% 4,4-diphenylazobenzene/95% celecoxib can show highly increased density and enhanced kinetic stability as compared to the liquid-cooled glass mixture. Our present work generalizes these results to mixtures with large ΔT_g values outside the dilute regime. Recently, two works

studied the stability of PVD glass mixtures of organic semiconductors. Cheng et al.¹⁶ reported that 50:50 codeposited glass mixtures of TPD and m-MTADATA formed highly stable glasses. The authors pointed out that small values of ΔT_g ($= 18$ K) and the ideal solution behavior between these two organic semiconductors were likely reasons why this binary system behaves like a neat PVD glass; our present work shows that a small ΔT_g is not a prerequisite. Ki et al.⁴³ reported that codeposited glass mixtures of 8-hydroxyquinolinolato-lithium (LiQ) and 4,7-diphenyl-1,10-phenanthroline (BPhen) prepared at $T_{sub} = 0.80$ – $0.89T_{g,mixture}$ did not show ultrastable behavior. We note that they also reported that pure LiQ failed to form stable glasses via PVD. The inability of LiQ to form stable glasses via PVD could be interpreted as a lack of surface mobility, which then might explain why LiQ/BPhen mixtures do not form stable glasses. This is a key difference from the six mixtures studied here, whose components can individually form stable glasses via PVD.

Molecular Orientation in Codeposited Semiconductor Glasses. In Figure 5, we demonstrate that $T_{sub}/T_{g,mixture}$ is the key factor controlling the birefringence of PVD organic semiconductor glass mixtures. We studied six codeposited systems in a broad substrate temperature range from $0.75T_{g,mixture}$ to $1.02T_{g,mixture}$, in which molecular packing varies continuously from “face-on” to “edge-on” and to isotropic packing.

The observation that eq 1 can successfully predict the birefringence of the codeposited mixtures is significant, and we want to specify the two assumptions needed to derive this equation. First, we assume that mobility of a given molecule at the surface of the codeposited glass is determined only by $T_{sub}/T_{g,mixture}$ for any composition of the glass. This assumption naturally leads to the conclusion that the two components will have similar mobilities during codeposition, as we inferred above based upon the ultrastability of codeposited mixtures with large ΔT_g . Second, we assume that a given surface mobility always leads to the same molecular orientation at the surface independent of the composition of the surface. We have no independent argument for the validity of this assumption, beyond the observation that eq 1 is quite accurate, and we do not know how to derive this equation without this assumption. eq 1 is a generalization of a relation proposed earlier by Jiang et al.³³ to explain the birefringence of the PVD glasses of DSA-Ph/Alq3, where PVD glasses of pure Alq3 have no birefringence.⁴⁴

We wish to emphasize that eq 1 is not a simple statement that the codeposited mixture at a specific T_{sub} will have the average birefringence of the two pure components deposited at the same T_{sub} . We show here that such a simple average does not describe the experimental data. If a simple average was valid, then at a given T_{sub} , we would have

$$\Delta n_{AB}(T_{sub}) = \varphi_A \times \Delta n_A(T_{sub}) + \varphi_B \times \Delta n_B(T_{sub}) \quad (2)$$

A comparison of our experimental data (red spheres) with the birefringence predicted from eq 2 (gray dashed lines) is shown in Figure 5. While some systems are reasonably described by eq 2, at least three mixtures are poorly described. The success of eq 1 and the failure of eq 2 indicate the key role for $T_{sub}/T_{g,mixture}$ in determining molecular orientation in codeposited glasses, which in turn signals the importance of mobility for this process, as anticipated by the surface equilibration mechanism. In more detail, it suggests that the two assumptions used to derive eq 1 are correct, at least for

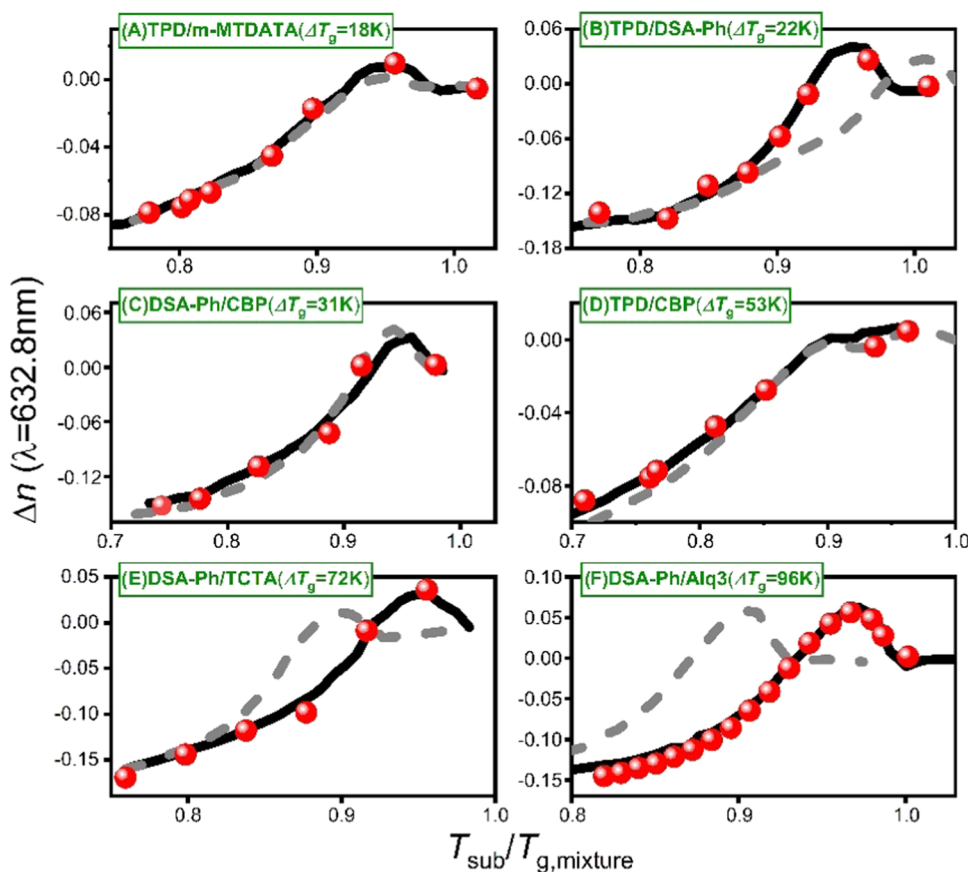


Figure 5. Birefringence of codeposited glass mixtures of organic semiconductors at wavelength $\lambda = 632.8$ nm. The red spheres denote the experimental birefringence determined from spectroscopic ellipsometry, while the black solid lines represent the predicted birefringence from eq 1. The gray dashed lines represent the predicted birefringence in eq 2. The birefringence data of single-component PVD glasses used to perform these calculations are displayed in Figure S6.

450 organic semiconductor mixtures similar to the six systems
 451 studied here. The success of eq 1 also implies that the
 452 birefringence contribution of each component in the mixture is
 453 individually described by our approach. Thus, we can also use
 454 this approach to understand the molecular orientation of each
 455 component in the mixture.

456 Our work complements and extends recent studies on the
 457 molecular orientation of emitters in PVD glass mixtures of
 458 organic semiconductors, with the goal of increasing device
 459 efficiency. Brutting et al. studied the orientation of a coumarin
 460 dye²³ and four nonpolar dyes⁴⁵ in a series of dye-doped guest–
 461 host systems deposited at room temperature and observed
 462 increasing horizontal orientation of the dye with decreasing
 463 $T_{\text{sub}}/T_{\text{g,host}}$. Since $T_{\text{g,host}}$ is expected to be quite close to
 464 $T_{\text{g,mixture}}$ in the case of dilute mixtures, their work indicates that
 465 the $T_{\text{sub}}/T_{\text{g,mixture}}$ controls the molecular orientation of emitters
 466 in dilute mixtures. Moreover, utilizing three different substrate
 467 temperatures, Komino et al.²⁵ observed that a linear dopant
 468 molecule in a host matrix of 3,3'-di(9H-carbazol-9-yl)-1,1'-
 469 biphenyl (mCBP) had a greater tendency to orient horizontally
 470 at lower substrate temperatures. Although these previous
 471 papers focused on dilute mixtures and studied at most three
 472 substrate temperatures, their results are consistent with our
 473 conclusion that $T_{\text{sub}}/T_{\text{g,mixture}}$ is the key factor controlling the
 474 molecular orientation in vapor-deposited glass mixtures.
 475 Because a wide range of substrate temperatures and nondilute
 476 mixtures were investigated in our work, we uncovered a larger
 477 pattern in molecular orientation that extends to both

478 components and applies to the entire range of possible
 479 compositions.

480 The result reported here may be useful for understanding
 481 the surface potential of vapor-deposited organic semiconduc-
 482 tors, which plays a key role in controlling charge
 483 injections.^{46–48} When polar molecules are deposited, any net
 484 alignment of the dipole moments (relative to the surface
 485 normal) can lead to a giant surface potential (GSP), which can
 486 exceed 15 V for 100 nm of deposited glass.⁴⁹ Recent work by
 487 Adachi and co-workers⁵⁰ showed that fluorine groups can be
 488 used to direct dipole orientation at the surface during
 489 deposition, leading to the production of glass films with either
 490 positively or negatively charged surfaces. As indicated in ref 50,
 491 this result strongly supports the surface equilibration
 492 mechanism at a qualitative level. Very recently, He et al.³⁰
 493 reported that the deposition rate can be used to control the
 494 GSP of pure organic semiconductors and 50:50 mixtures, in
 495 qualitative accord with the surface equilibration mechanism.
 496 These authors reported that the GSP for codeposited glasses
 497 was approximately the average GSP for pure materials. We
 498 speculate that over a broad range of deposition conditions, a
 499 more accurate prediction for GSP for mixtures might be
 500 obtained by averaging GSP values at the same value of $T_{\text{sub}}/T_{\text{g,mixture}}$,
 501 in analogy to eq 1. In some studies, mixtures of polar
 502 and nonpolar molecules have been used to optimize GSP,^{31,51}
 503 and thus, our observation that polar/nonpolar pairs of
 504 molecules form ultrastable glasses is relevant for future work.
 505 It should be noted that GSP and birefringence characterize

506 different aspects of anisotropic packing, even in the case where
507 the dipole moment is aligned with the polarizability tensor. In
508 our view, the surface equilibration mechanism should generally
509 describe all of the measures of anisotropy in PVD glasses.

510 **Generality of These Results.** Given the importance of
511 codeposited PVD glasses of organic semiconductors, it is useful
512 to consider how general our results may be. We emphasize that
513 the mixtures of organic semiconductors studied here are
514 diverse: (1) covering various combinations of molecular
515 shapes, e.g., TPD/m-MTADATA (rod/disk), TPD/DSA-Ph
516 (rod/rod), and DSA-Ph/Alq3 (rod/sphere); (2) spanning a
517 wide range of ΔT_g in components from 18 K (TPD/m-
518 MTADATA) to 96 K (DSA-Ph/Alq3); and (3) including
519 mixtures of nonpolar/nonpolar (TPD/CBP) and nonpolar/
520 polar (DSA-Ph/Alq3) molecules.

521 Based upon these results, we anticipate that if two organic
522 semiconductors meet two key criteria, the codeposited glass
523 mixtures formed by them will exhibit ultrastability when
524 deposited at $T_{sub} = 0.78-0.88T_{g,mixture}$: (1) the organic
525 semiconductors can form ultrastable glasses as pure compo-
526 nents and (2) the two components are well mixed in the glass
527 (but without strong association). In addition, the molecular
528 orientation of each component in the PVD glass mixtures can
529 be predicted as shown in [eq 1](#). We anticipate that [eq 1](#) is
530 applicable to binary mixtures with compositions other than
531 50:50 (e.g., the dilute mixtures that are commonly utilized in
532 OLEDs) if the two components mix well and show the ability
533 to individually form ultrastable PVD glasses.

534 ■ SUMMARY

535 The current work conducts a thorough investigation on the
536 kinetic stability, enthalpy, and molecular orientation of six
537 codeposited 50:50 glass mixtures of organic semiconductors.
538 The organic semiconductor mixtures studied here are diverse
539 with ΔT_g ranging from 18 to 96 K and covering various
540 combinations of molecular shape and polarity. Nevertheless, all
541 six systems exhibit high kinetic stability and significantly
542 reduced enthalpy when deposited at $T_{sub} = 0.78-0.88T_{g,mixture}$,
543 compared to their corresponding liquid-cooled glassy mixtures.
544 Furthermore, the birefringence of codeposited organic semi-
545 conductor glass mixtures is quantitatively predictable based on
546 the birefringence of the corresponding single-component PVD
547 glasses using a mixing rule ([eq 1](#)) derived from the surface
548 equilibration mechanism.

549 We expect that these findings will extend to other
550 codeposited organic semiconductor glass mixtures, even
551 those with compositions other than 50:50 (including dilute
552 mixtures), if the two components can individually form PVD
553 stable glasses and mix well during deposition. Consequently, a
554 generic approach is proposed for producing highly stable PVD
555 organic semiconductor glass mixtures and manipulating their
556 molecular packing.

557 Physical vapor-deposited glass mixtures of organic semi-
558 conductors are generally utilized as light-emitting layers in the
559 formation of OLEDs. Our findings are significant for designing
560 electronic devices with increased device lifetime and opera-
561 tional efficiency. Our work indicates that for a given organic
562 semiconductor blend with room temperature deposition (i.e.,
563 298 K), the most stable glass mixtures will be produced when
564 the glass-transition temperature of the mixture is around 340–
565 370 K, which is a criterion to manipulate the composition.
566 Furthermore, our work shows that dilute mixtures with
567 ultrastability for room temperature deposition will be obtained

568 when the T_g of host compounds is 340–370 K. Previous work 569
has shown that OLED devices prepared from ultrastable 569
glasses can have substantially longer device lifetimes,⁹ and thus, 570
our new results provide guidance for device design. In addition, 571
for a given pair of organic semiconductors, our work provides 572
guidance on selecting an appropriate composition to obtain 573
horizontal molecular orientation for room temperature 574
deposition, which maximizes device efficiency. 575

576 ■ ASSOCIATED CONTENT

577 ■ Supporting Information

578 The Supporting Information is available free of charge at 578
<https://pubs.acs.org/doi/10.1021/acs.chemmater.3c02935>. 579

580 (1) DSC results for bulk organic semiconductors 580
(Figure S1); (2) DSC results for 50:50 bulk mixtures 581
of organic semiconductors (Figure S2); (3) prediction 582
of the specific heat capacity of 50:50 DSA-Ph/Alq3 583
mixture close to the glass transition (Figure S3); (4) 584
comparison of the DSC data of codeposited TPD/DSA- 585
Ph at $T_{sub} = 300$ K in two separate depositions; (5) 586
comparison of experimental $T_{g,mixture}$ of TPD/CBP and 587
TPD/m-MTADATA with the theoretical model; (6) the 588
birefringence of single-component PVD glasses of 589
studied organic semiconductors ([PDF](#)) 590

591 ■ AUTHOR INFORMATION

592 Corresponding Author

593 **Mark D. Ediger** – *Department of Chemistry, University of*
594 *Wisconsin-Madison, Madison, Wisconsin 53706, United*
595 *States; orcid.org/0000-0003-4715-8473;*
596 *Email: ediger@chem.wisc.edu*

597 Authors

598 **Shinian Cheng** – *Department of Chemistry, University of*
599 *Wisconsin-Madison, Madison, Wisconsin 53706, United*
600 *States; orcid.org/0000-0002-5615-8646*

601 **Yeung Lee** – *Department of Chemistry, University of*
602 *Wisconsin-Madison, Madison, Wisconsin 53706, United*
603 *States; orcid.org/0000-0002-0179-395X*

604 **Junguang Yu** – *School of Pharmacy, University of Wisconsin-*
605 *Madison, Madison, Wisconsin 53705, United States;*
606 *orcid.org/0000-0001-6458-8307*

607 **Lian Yu** – *School of Pharmacy, University of Wisconsin-*
608 *Madison, Madison, Wisconsin 53705, United States;*
609 *orcid.org/0000-0002-4253-5658*

610 Complete contact information is available at:

611 <https://pubs.acs.org/doi/10.1021/acs.chemmater.3c02935>

612 Author Contributions

613 This manuscript was written through contributions of all 613
614 authors. All authors have given approval to the final version of 614
the manuscript. 615

616 Notes

617 The authors declare no competing financial interest.

618 ■ ACKNOWLEDGMENTS

619 Work by S.C., J.Y., L.Y., and M.D.E. was supported by the NSF 619
620 through the University of Wisconsin Materials Research 620
621 Science and Engineering Center (DMR-2309000). Work by 621
622 Y.L. was supported by the U.S. Department of Energy, Office 622
623 of Basic Energy Sciences, Division of Materials Sciences and 623
Engineering, DE-SC0002161. 624

625 ■ REFERENCES

626 (1) Pode, R. Organic light emitting diode devices: An energy 627 efficient solid state lighting for applications. *Renewable Sustainable* 628 *Energy Rev.* **2020**, *133*, No. 110043, DOI: 10.1016/j.rser.2020.110043.

629 (2) Hodge, I. M. Physical aging in polymer glasses. *Science* **1995**, *267* 630 (5206), 1945–1947.

631 (3) Han, E.-M.; Do, L.-M.; Yamamoto, N.; Fujihira, M. 632 Crystallization of organic thin films for electroluminescent devices. 633 *Thin Solid Films* **1996**, *273* (1–2), 202–208.

634 (4) Scholz, S.; Kondakov, D.; Lussem, B.; Leo, K. Degradation 635 Mechanisms and Reactions in Organic Light-Emitting Devices. *Chem.* 636 *Rev.* **2015**, *115* (16), 8449–8503.

637 (5) Swallen, S. F.; Kearns, K. L.; Mapes, M. K.; Kim, Y. S.; 638 McMahon, R. J.; Ediger, M. D.; Wu, T.; Yu, L.; Satija, S. Organic 639 glasses with exceptional thermodynamic and kinetic stability. *Science* 640 **2007**, *315* (5810), 353–356.

641 (6) Raegen, A. N.; Yin, J.; Zhou, Q.; Forrest, J. A. Ultrastable 642 monodisperse polymer glass formed by physical vapour deposition. 643 *Nat. Mater.* **2020**, *19* (10), 1110–1113.

644 (7) Bagchi, K.; Fiori, M. E.; Bishop, C.; Toney, M. F.; Ediger, M. D. 645 Stable Glasses of Organic Semiconductor Resist Crystallization. *J.* 646 *Phys. Chem. B* **2021**, *125* (1), 461–466.

647 (8) Rodriguez-Tinoco, C.; Gonzalez-Silveira, M.; Ramos, M. A.; 648 Rodriguez-Viejo, J. Ultrastable glasses: new perspectives for an old 649 problem. *Riv. Nuovo Cimento* **2022**, *45* (5), 325–406.

650 (9) Ràfols-Ribé, J.; Will, P.-A.; Hänisch, C.; Gonzalez-Silveira, M.; 651 Lenk, S.; Rodriguez-Viejo, J.; Reineke, S. High-performance organic 652 light-emitting diodes comprising ultrastable glass layers. *Sci. Adv.* 653 **2018**, *4* (5), No. eaar8332, DOI: 10.1126/sciadv.aar8332.

654 (10) Liu, T.; Exarhos, A. L.; Alguire, E. C.; Gao, F.; Salami- 655 Ranjbaran, E.; Cheng, K.; Jia, T.; Subotnik, J. E.; Walsh, P. J.; 656 Kikkawa, J. M.; Fakhraai, Z. Birefringent stable glass with 657 predominantly isotropic molecular orientation. *Phys. Rev. Lett.* **2017**, 658 *119* (9), No. 095502, DOI: 10.1103/PhysRevLett.119.095502.

659 (11) Gujral, A.; Yu, L.; Ediger, M. D. Anisotropic organic glasses. 660 *Curr. Opin. Solid State Mater. Sci.* **2018**, *22* (2), 49–57.

661 (12) Dalal, S. S.; Fakhraai, Z.; Ediger, M. D. High-Throughput 662 Ellipsometric Characterization of Vapor-Deposited Indomethacin 663 Glasses. *J. Phys. Chem. B* **2013**, *117* (49), 15415–15425.

664 (13) Dalal, S. S.; Walters, D. M.; Lyubimov, I.; de Pablo, J. J.; Ediger, 665 M. D. Tunable molecular orientation and elevated thermal stability of 666 vapor-deposited organic semiconductors. *Proc. Natl. Acad. Sci. U.S.A.* 667 **2015**, *112* (14), 4227–4232.

668 (14) Luo, P.; Fakhraai, Z. Surface-Mediated Formation of Stable 669 Glasses. *Annu. Rev. Phys. Chem.* **2023**, *74*, 361–389.

670 (15) Kasting, B. J.; Gabriel, J. P.; Tracy, M. E.; Guiseppi-Elie, A.; 671 Richert, R.; Ediger, M. D. Unusual Transformation of Mixed Isomer 672 Decahydroisoquinoline Stable Glasses. *J. Phys. Chem. B* **2023**, *127* 673 (26), 5948–5958.

674 (16) Cheng, S.; Lee, Y.; Yu, J.; Yu, L.; Ediger, M. D. Surface 675 Equilibration Mechanism Controls the Stability of a Model 676 Codeposited Glass Mixture of Organic Semiconductors. *J. Phys.* 677 *Chem. Lett.* **2023**, *14* (18), 4297–4303.

678 (17) Jankus, V.; Data, P.; Graves, D.; McGuinness, C.; Santos, J.; 679 Bryce, M. R.; Dias, F. B.; Monkman, A. P. Highly efficient TADF 680 OLEDs: how the emitter–host interaction controls both the excited 681 state species and electrical properties of the devices to achieve near 682 100% triplet harvesting and high efficiency. *Adv. Funct. Mater.* **2014**, 683 *24* (39), 6178–6186.

684 (18) Flämmich, M.; Frischeisen, J.; Setz, D. S.; Michaelis, D.; 685 Krummacher, B. C.; Schmidt, T. D.; Brüttling, W.; Danz, N. Oriented 686 phosphorescent emitters boost OLED efficiency. *Org. Electron.* **2011**, 687 *12* (10), 1663–1668.

688 (19) Kim, S. Y.; Jeong, W. I.; Mayr, C.; Park, Y. S.; Kim, K. H.; Lee, 689 J. H.; Moon, C. K.; Brüttling, W.; Kim, J. J. Organic Light-Emitting 690 diodes with 30% external quantum efficiency based on a horizontally 691 oriented emitter. *Adv. Funct. Mater.* **2013**, *23* (31), 3896–3900.

692 (20) Mayr, C.; Lee, S. Y.; Schmidt, T. D.; Yasuda, T.; Adachi, C.; 693 Brüttling, W. Efficiency Enhancement of Organic Light-Emitting 694 Diodes Incorporating a Highly Oriented Thermally Activated Delayed 695 Fluorescence Emitter. *Adv. Funct. Mater.* **2014**, *24* (33), 5232–5239. 696

697 (21) Yokoyama, D. Molecular orientation in small-molecule organic 698 light-emitting diodes. *J. Mater. Chem.* **2011**, *21* (48), 19187–19202. 699

700 (22) Tenopala-Carmona, F.; Lee, O. S.; Crovini, E.; Neferu, A. M.; 701 Murawski, C.; Olivier, Y.; Zysman-Colman, E.; Gather, M. C. 702 Identification of the Key Parameters for Horizontal Transition Dipole 703 Orientation in Fluorescent and TADF Organic Light-Emitting 704 Diodes. *Adv. Mater.* **2021**, *33* (37), No. 2100677, DOI: 10.1002/adma.202100677. 705

706 (23) Mayr, C.; Brüttling, W. Control of Molecular Dye Orientation 707 in Organic Luminescent Films by the Glass Transition Temperature 708 of the Host Material. *Chem. Mater.* **2015**, *27* (8), 2759–2762. 709

710 (24) Tanaka, M.; Noda, H.; Nakanotani, H.; Adachi, C. Molecular 711 orientation of disk-shaped small molecules exhibiting thermally 712 activated delayed fluorescence in host–guest films. *Appl. Phys. Lett.* 713 **2020**, *116* (2), No. 023302, DOI: 10.1063/1.5140210. 714

715 (25) Komino, T.; Tanaka, H.; Adachi, C. Selectively controlled 716 orientational order in linear-shaped thermally activated delayed 717 fluorescent dopants. *Chem. Mater.* **2014**, *26* (12), 3665–3671. 718

719 (26) Jurow, M. J.; Mayr, C.; Schmidt, T. D.; Lampe, T.; Djurovich, 720 P. I.; Brüttling, W.; Thompson, M. E. Understanding and predicting 721 the orientation of heteroleptic phosphors in organic light-emitting 722 materials. *Nat. Mater.* **2016**, *15* (1), 85–91. 723

724 (27) Ito, E.; Washizu, Y.; Hayashi, N.; Ishii, H.; Matsui, N.; Tsuboi, 725 K.; Ouchi, Y.; Harima, Y.; Yamashita, K.; Seki, K. Spontaneous 726 buildup of giant surface potential by vacuum deposition of Alq 3 and 727 its removal by visible light irradiation. *J. Appl. Phys.* **2002**, *92* (12), 728 7306–7310. 729

729 (28) Noguchi, Y.; Tanaka, Y.; Ishii, H.; Brüttling, W. Understanding 730 spontaneous orientation polarization of amorphous organic semi- 731 conducting films and its application to devices. *Synth. Met.* **2022**, *288*, 732 No. 117101, DOI: 10.1016/j.synthmet.2022.117101. 733

733 (29) Hofmann, A.; Schmid, M.; Brüttling, W. The many facets of 734 molecular orientation in organic optoelectronics. *Adv. Opt. Mater.* **2021**, *9* (21), 735 No. 2101004, DOI: 10.1002/adom.202101004. 736

736 (30) He, S.; Pakhomenko, E.; Holmes, R. J. Process Engineered 737 Spontaneous Orientation Polarization in Organic Light-Emitting 738 Devices. *ACS Appl. Mater. Interfaces* **2023**, *15* (1), 1652–1660. 739

740 (31) Cakaj, A.; Schmid, M.; Hofmann, A.; Brüttling, W. Controlling 741 Spontaneous Orientation Polarization in Organic Semiconductors- 742 The Case of Phosphine Oxides. *ACS Appl. Mater. Interfaces* **2023**, *15* (47), 743 54721–54731. 744

744 (32) Van den Brande, N.; Gujral, A.; Huang, C. B.; Bagchi, K.; 745 Hofstetter, H.; Yu, L.; Ediger, M. D. Glass Structure Controls Crystal 746 Polymorph Selection in Vapor-Deposited Films of 4,4'-Bis(N- 747 carbazolyl)-1,1'-biphenyl. *Cryst. Growth Des.* **2018**, *18* (10), 5800– 748 5807. 749

750 (33) Jiang, J.; Walters, D. M.; Zhou, D.; Ediger, M. D. Substrate 751 temperature controls molecular orientation in two-component vapor- 752 deposited glasses. *Soft Matter* **2016**, *12* (13), 3265–3270. 753

754 (34) Zhang, Y.; Fakhraai, Z. Invariant Fast Diffusion on the Surfaces 755 of Ultrastable and Aged Molecular Glasses. *Phys. Rev. Lett.* **2017**, *118* (6), 756 No. 066101, DOI: 10.1103/PhysRevLett.118.066101. 757

758 (35) Kearns, K. L.; Swallen, S. F.; Ediger, M. D.; Wu, T.; Sun, Y.; Yu, 759 L. Hiking down the energy landscape: Progress toward the Kauzmann 760 temperature via vapor deposition. *J. Phys. Chem. B* **2008**, *112* (16), 761 4934–4942. 762

762 (36) Pérez-Castañeda, T.; Jiménez-Riobóo, R. J.; Ramos, M. A. 763 Two-level systems and boson peak remain stable in 110-million-year- 764 old amber glass. *Phys. Rev. Lett.* **2014**, *112* (16), No. 165901, 765 DOI: 10.1103/PhysRevLett.112.165901. 766

767 (37) Zhao, J.; Simon, S. L.; McKenna, G. B. Using 20-million-year- 768 old amber to test the super-Arrhenius behaviour of glass-forming 769 systems. *Nat. Commun.* **2013**, *4* (1), No. 1783. 770

771 (38) Walters, D. M.; Antony, L.; de Pablo, J. J.; Ediger, M. D. 772 Influence of Molecular Shape on the Thermal Stability and Molecular 773

762 Orientation of Vapor-Deposited Organic Semiconductors. *J. Phys. Chem. Lett.* **2017**, *8* (14), 3380–3386.

763 (39) Tsuchiya, Y.; Nakamura, N.; Kakumachi, S.; Kusuhara, K.; Chan, C.-Y.; Adachi, C. A convenient method to estimate the glass transition temperature of small organic semiconductor materials. *Chem. Commun.* **2022**, *58* (80), 11292–11295.

764 (40) Zhang, W.; Teerakapibal, R.; Yu, L. Surface Mobility of Amorphous o-Terphenyl: A Strong Inhibitory Effect of Low-Concentration Polystyrene. *J. Phys. Chem. B* **2016**, *120* (27), 6842–6847.

765 (41) Whitaker, K. R.; Scifo, D. J.; Ediger, M. D.; Ahrenberg, M.; Schick, C. Highly Stable Glasses of cis-Decalin and cis/trans-Decalin Mixtures. *J. Phys. Chem. B* **2013**, *117* (42), 12724–12733.

766 (42) Qiu, Y.; Antony, L. W.; Torkelson, J. M.; de Pablo, J. J.; Ediger, M. D. Tenfold increase in the photostability of an azobenzene guest in vapor-deposited glass mixtures. *J. Chem. Phys.* **2018**, *149* (20), No. 204503, DOI: [10.1063/1.5052003](https://doi.org/10.1063/1.5052003).

767 (43) Ki, M. S.; Sim, M.; Kwon, O.; Im, K.; Choi, B.; Cha, B. J.; Kim, Y. D.; Jin, T. Y.; Paeng, K. Improved Thermal Stability and Operational Lifetime of Blue Fluorescent Organic Light-Emitting Diodes by Using a Mixed-Electron Transporting Layer. *ACS Mater. Lett.* **2022**, *4* (9), 1676–1683.

768 (44) Bagchi, K.; Jackson, N. E.; Gujral, A.; Huang, C. B.; Toney, M. F.; Yu, L.; de Pablo, J. J.; Ediger, M. D. Origin of Anisotropic Molecular Packing in Vapor-Deposited Alq₃ Glasses. *J. Phys. Chem. Lett.* **2019**, *10* (2), 164–170.

769 (45) Nguyen, B. M.; Schmid, M.; Kirsch, J.; Cakaj, A.; Brüting, W. On the Orientation Mechanism of Nonpolar Dyes in Light-Emitting Guest-Host Systems. *Chem. Mater.* **2023**, *35* (17), 7333–7343.

770 (46) Isoshima, T.; Okabayashi, Y.; Ito, E.; Hara, M.; Chin, W. W.; Han, J. W. Negative giant surface potential of vacuum-evaporated tris [7-propyl-8-hydroxyquinolinolato] aluminum (III)[Al (7-Prq) 3] film. *Org. Electron.* **2013**, *14* (8), 1988–1991.

771 (47) Pakhomenko, E.; He, S.; Holmes, R. J. Understanding and engineering spontaneous orientation polarization in organic light-emitting devices. *Chem. Phys. Rev.* **2023**, *4* (2), No. 021308, DOI: [10.1063/5.0141588](https://doi.org/10.1063/5.0141588).

772 (48) Noguchi, Y.; Ishii, H.; Jäger, L.; Schmidt, T. D.; Brüting, W. Spontaneous Orientation Polarization in Organic Light-Emitting Diodes and its Influence on Charge Injection, Accumulation, and Degradation Properties. *Org. Semicond. Optoelectron.* **2021**, 273–293.

773 (49) Noguchi, Y.; Miyazaki, Y.; Tanaka, Y.; Sato, N.; Nakayama, Y.; Schmidt, T. D.; Brüting, W.; Ishii, H. Charge accumulation at organic semiconductor interfaces due to a permanent dipole moment and its orientational order in bilayer devices. *J. Appl. Phys.* **2012**, *111* (11), No. 114508, DOI: [10.1063/1.4724349](https://doi.org/10.1063/1.4724349).

774 (50) Tanaka, M.; Auffray, M.; Nakanotani, H.; Adachi, C. Spontaneous formation of metastable orientation with well-organized permanent dipole moment in organic glassy films. *Nat. Mater.* **2022**, *21* (7), 819–825.

775 (51) Hofmann, A. J.; Züfle, S.; Shimizu, K.; Schmid, M.; Wessels, V.; Jäger, L.; Altazin, S.; Ikegami, K.; Khan, M. R.; Neher, D.; et al. Dipolar doping of organic semiconductors to enhance carrier injection. *Phys. Rev. Appl.* **2019**, *12* (6), No. 064052, DOI: [10.1103/PhysRevApplied.12.064052](https://doi.org/10.1103/PhysRevApplied.12.064052).